Numerical Methods for Solid Mechanics on Overlapping Grids

Jeffrey W. Banks

Lawrence Livermore National Laboratory

Overset Composite Grids and Solution Technology
Moffett Field, September 21, 2008

Collaborators

William Henshaw
Center for Applied Scientific Computing
Lawrence Livermore National Laboratory

Donald Schwendeman
Department of Mathematical Sciences
Rensselaer Polytechnic Institute

Support
Department of Energy
National Science Foundation

Motivation for this work

Solid mechanics capability for high-speed fluid structure problems

- e.g. explosive rate stick

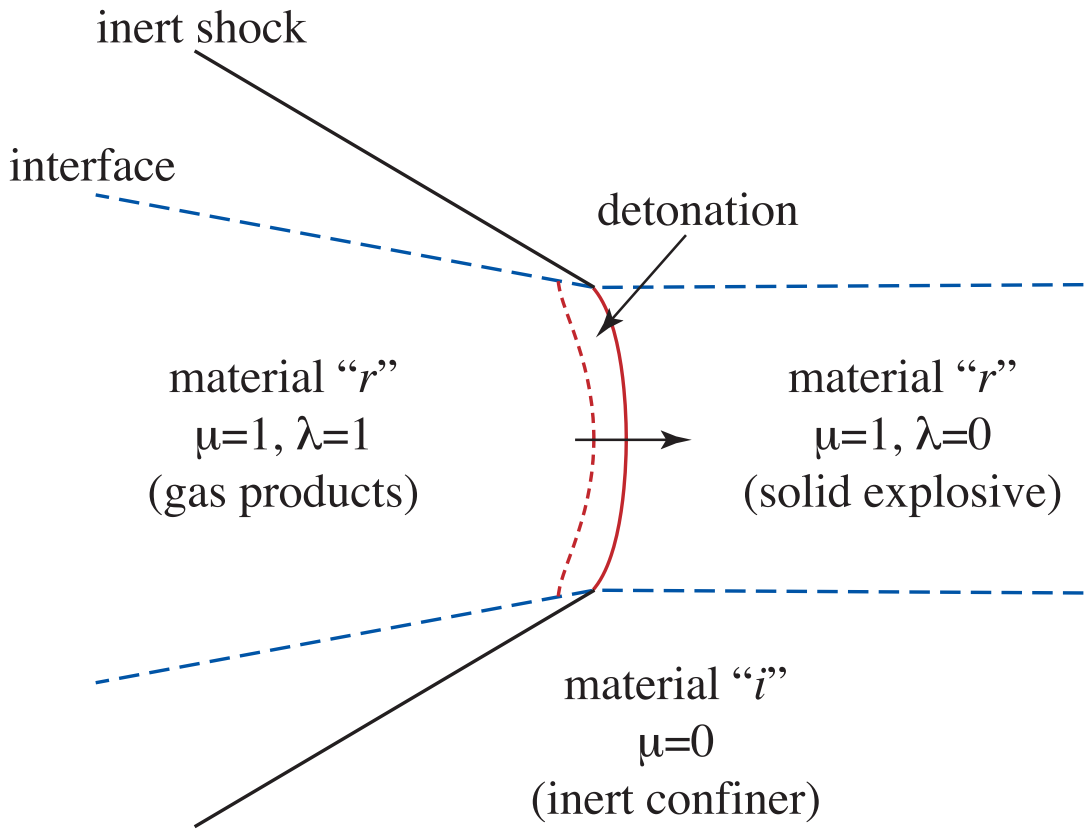

- Previous work with overset grids
  - high-speed fluid mechanics (with and without reaction)
  - multiphase models of high explosives
  - two fluid approximations for confinement
  - moving and deforming geometries
  - conjugate heat transfer

- We need a overset solid mechanics capability

Governing Equations

We wish to compare first and second order formulations of the equations of linear elasticity

- Second order system for the displacements

$$\rho \frac{\partial^2 u_i}{\partial t^2} = \frac{\partial \sigma_{ij}}{\partial x_j} + \rho f_i, \qquad \mathbf{x} \in \Omega, \quad t > 0, \quad i = 1, 2, \ldots, N_d$$

  - with stress tensor

$$\sigma_{ij} = \lambda \left(\epsilon_{kk} \right) \delta_{ij} + 2\mu \epsilon_{ij}, \qquad \epsilon_{ij} = \frac{1}{2} \left(\frac{\partial u_i}{\partial x_j} + \frac{\partial u_j}{\partial x_i} \right)$$

- First order system in velocity and stress

$$\left.\begin{aligned} \frac{\partial u_i}{\partial t} &= v_i, \\ \frac{\partial v_i}{\partial t} &= \frac{1}{\rho} \frac{\partial \sigma_{ij}}{\partial x_j} + f_i, \\ \frac{\partial \sigma_{ij}}{\partial t} &= \lambda \left(\dot{\epsilon}_{kk} \right) \delta_{ij} + 2\mu \dot{\epsilon}_{ij}, \end{aligned}\right\} \qquad \mathbf{x} \in \Omega, \quad t > 0, \quad i = 1, 2, \ldots, N_d$$

Boundary and Initial Conditions

- Initial conditions for displacements and velocities

$$\mathbf{u}(\mathbf{x},0) = \mathbf{u}_0(\mathbf{x}), \qquad \frac{\partial \mathbf{u}}{\partial t}(\mathbf{x},0) = \mathbf{v}_0(\mathbf{x}), \qquad \mathbf{x} \in \Omega$$

- Initial stress derived from positions

- We consider a variety of boundary conditions

$$\begin{aligned}
&\mathbf{u} = \mathbf{g}_d(\mathbf{x},t), && \text{displacement boundary condition,}\\
&\mathbf{n}\cdot\sigma = \mathbf{g}_t(\mathbf{x},t), && \text{traction boundary condition,}\\
&\left.\begin{aligned}\mathbf{n}\cdot\mathbf{u} &= g_s(\mathbf{x},t)\\ \mathbf{n}\cdot\sigma\cdot\tau_\alpha &= g_{s,\alpha}(\mathbf{x},t)\end{aligned}\right\} && \text{slip-wall boundary conditions.}
\end{aligned}$$

- A few notable items:
  - The first and second order systems are compatible under certain constraints
    - Saint-Venant compatibility condition
  - The first order system maintains positions in addition to velocities and stress
    - stress and position are coupled at domain boundaries
    - relaxation can be used to directly enforce interior compatibility

Second Order System (SOS) Discretization

- The equations are discretized using 2nd order centered finite differences
- Summation by parts gives stability for a single curvilinear grid
- Grid overlap can lead to instabilities
  - artificial dissipation (typically $d = 4$)

$$\mathcal{D}_h^d \mathbf{u}_\mathbf{i}^n = -\frac{\alpha_d}{h} \sum_{j=1}^{N_d} (-\Delta_{+j}\Delta_{-j})^{d/2} \left(\frac{\mathbf{u}_\mathbf{i}^n - \mathbf{u}_\mathbf{i}^{n-1}}{\Delta t} \right)$$

  - Filter (typically $d = 6$)

$$\mathbf{u}_\mathbf{i}^{n,*} = \mathcal{F}_d(\mathbf{u}_\mathbf{i}^n) = \mathbf{u}_\mathbf{i}^n - \beta_d \sum_{j=1}^{d} (-\Delta_{+j}\Delta_{-j})^{d/2} \mathbf{u}_\mathbf{i}^n$$

- with $\beta_d = \frac{1}{2^d n_d}$, the plus-minus mode is eliminated

  - A normal mode stability analysis motivates these choices

First Order System (FOS) Discretization

- The equations are discretized using a 2nd order conservative flux based scheme

$$\mathbf{w}_{\mathbf{i}}^{n+1} = \mathbf{w}_{\mathbf{i}}^{n} - \frac{\Delta t}{J_{\mathbf{i}}} \sum_{\alpha=1}^{N_d} D_{+\alpha}\, \mathbf{f}^{(\alpha)}_{\mathbf{i}-\frac{1}{2}\hat{\mathbf{e}}_\alpha} + \Delta t\, \mathbf{h}_{\mathbf{i}}^{n+1/2}$$

- Fluxes are found using an upwind (Godunov) method

$$\mathbf{f}^{(\alpha)}_{\mathbf{i}+\frac{1}{2}\hat{\mathbf{e}}_\alpha} = \frac{1}{2}\left(\mathbf{f}^{(\alpha)}(\mathbf{w}_R) + \mathbf{f}^{(\alpha)}(\mathbf{w}_L)\right) - E_\alpha^{\frac{1}{2}} \left[\frac{J_{\mathbf{i}}}{2} \sum_{m=1}^{n_c} \Gamma^{(m)}_{\alpha,\mathbf{i}} \left|K^{(m)}_{\alpha,\mathbf{i}}\right|^{(m)}_{\alpha,\mathbf{i}}\right]$$

- Reconstruction to cell faces gives left and right states for Riemann problem

$$\mathbf{w}_L = \mathbf{w}_{\mathbf{i}}^{n} + \frac{1}{2} Z_{\alpha,\mathbf{i}}\, \mathbf{a}_{\alpha,\mathbf{i}} - \sum_{j=1}^{N_d} \frac{\Delta t}{2\Delta r_j} Z_{j,\mathbf{i}} K_{j,\mathbf{i}}\, \mathbf{a}^{n}_{j,\mathbf{i}} + \frac{\Delta t}{2}\mathbf{h}_{\mathbf{i}}^{n},$$

$$\mathbf{w}_R = E_\alpha \left[\mathbf{w}_{\mathbf{i}}^{n} - \frac{1}{2} Z_{\alpha,\mathbf{i}}\, \mathbf{a}_{\alpha,\mathbf{i}} - \sum_{j=1}^{N_d} \frac{\Delta t}{2\Delta r_j} Z_{j,\mathbf{i}} K_{j,\mathbf{i}}\, \mathbf{a}^{n}_{j,\mathbf{i}} + \frac{\Delta t}{2}\mathbf{h}_{\mathbf{i}}^{n}\right].$$

Stability on Overlapping Grids

- Consider the second order wave equation on a semi-infinite domain $x \in (-\infty, b]$
- Discretize on an overlapping grid using second order centered differences

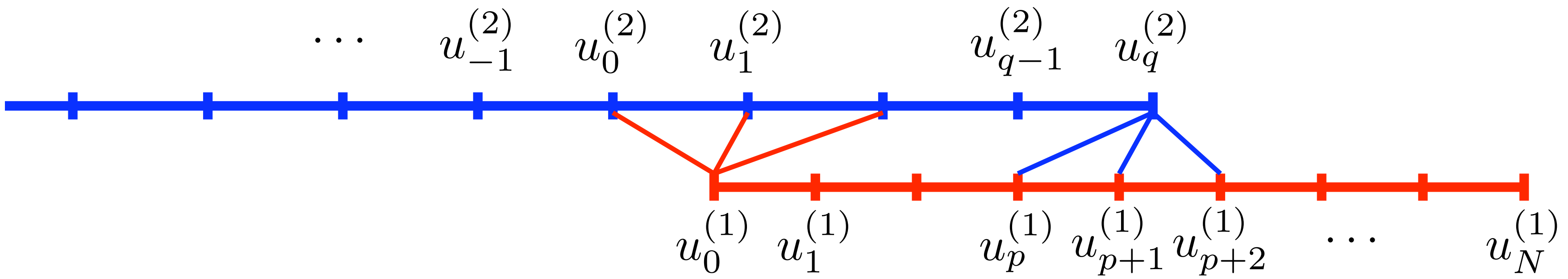

- Define stability to mean that the solution remains ***uniformly bounded*** in time
- Normal mode theory leads to the following eigenvalue problem

$$(sh_1)^2\tilde{u}_j^{(1)} = \tilde{u}_{j+1}^{(1)} - 2\tilde{u}_j^{(1)} + \tilde{u}_{j-1}^{(1)}, \quad j = 1, 2, \ldots, N-1,$$

$$(sh_2)^2\tilde{u}_j^{(2)} = \tilde{u}_{j+1}^{(2)} - 2\tilde{u}_j^{(2)} + \tilde{u}_{j-1}^{(2)}, \quad j = \ldots, q-2, q-1,$$

$$\tilde{u}_N^{(1)} = 0, \quad |\tilde{u}_j^{(2)}| < \infty,$$

$$\tilde{u}_0^{(1)} = \sum_{k=0}^{r} a_k \tilde{u}_k^{(2)}, \qquad \tilde{u}_q^{(2)} = \sum_{k=0}^{r} b_k \tilde{u}_{p+k}^{(1)}.$$

Stability (cont'd)

- Normal mode theory for the second order system says
  - Solutions to the eigenvalue problem grow as e^{st}
  - If $Re(s) > 0$, then by our definition the discretization is unstable
  - Assume a solution with parameters $(s, h_1, h_2, r, \alpha, \beta, N)$
    - Then there is a second solution with parameters $(s\gamma, h_1/\gamma, h_2/\gamma, r, \alpha, \beta, N)$
  - It is possible to find solutions numerically ... e.g.

$$h_1 = 1, \quad h_2 \approx 1.4445, \quad r = 2, \quad \alpha \approx 1.4408, \quad \beta \approx 1.2527, \quad p = 1, \quad q = 3, \quad N = 7$$

- Therefore the artificial dissipation parameter must grow with the mesh ... i.e.

$$\frac{\partial^2 u}{\partial t^2} = \frac{\partial^2 u}{\partial x^2} - \frac{a_d}{h}\Big(- h^2 \frac{\partial^2}{\partial x^2}\Big)^{/2} \frac{\partial u}{\partial t},$$

- A similar analysis is done for the FOS
  - The upwind dissipation has the correct form and naturally stabilizes the scheme

Experiments Concerning Stability

- Consider a planar disk discretized on an overlapping grid (both fixed, and narrow)
- Use method of analytic solutions to generate an exact solution

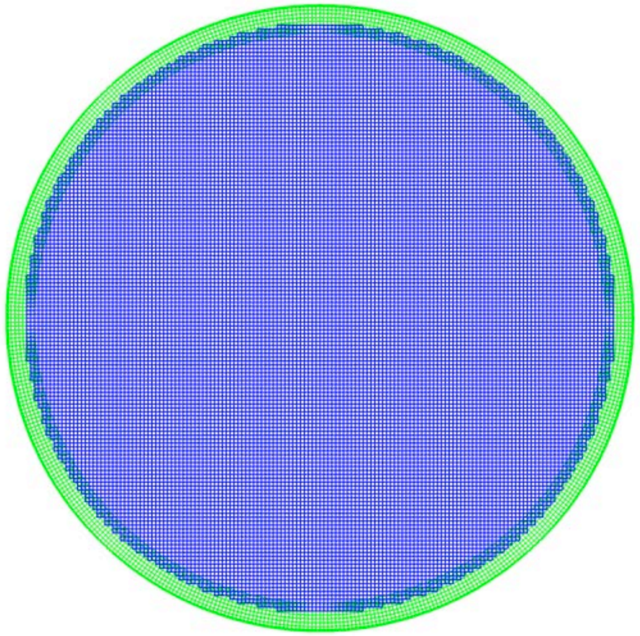

narrow boundary grid

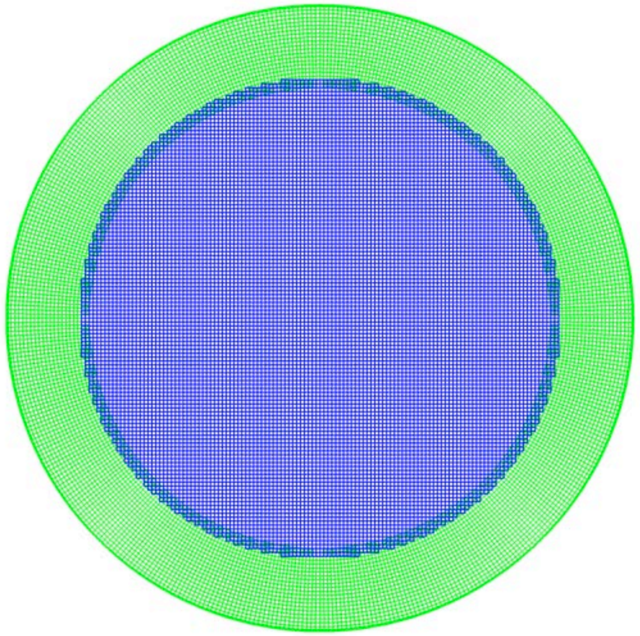

fixed width grid

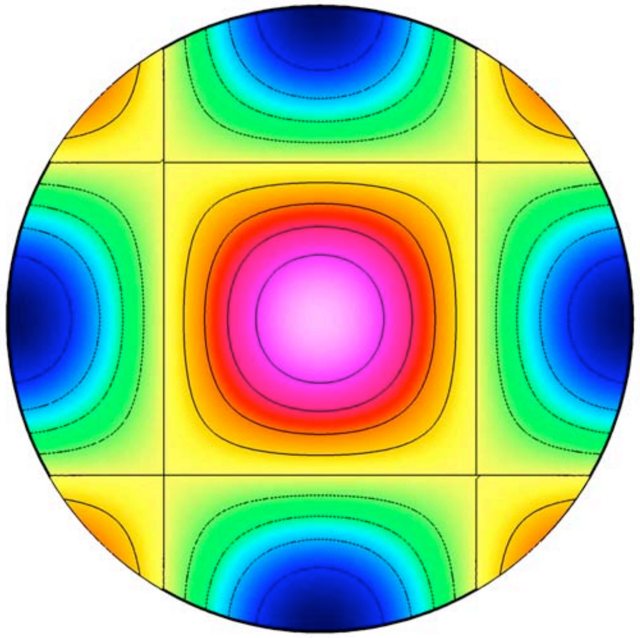

TZ solution

Experiments Concerning Stability

- Consider a planar disk discretized on an overlapping grid (both fixed, and narrow)
- Use method of analytic solutions to generate an exact solution

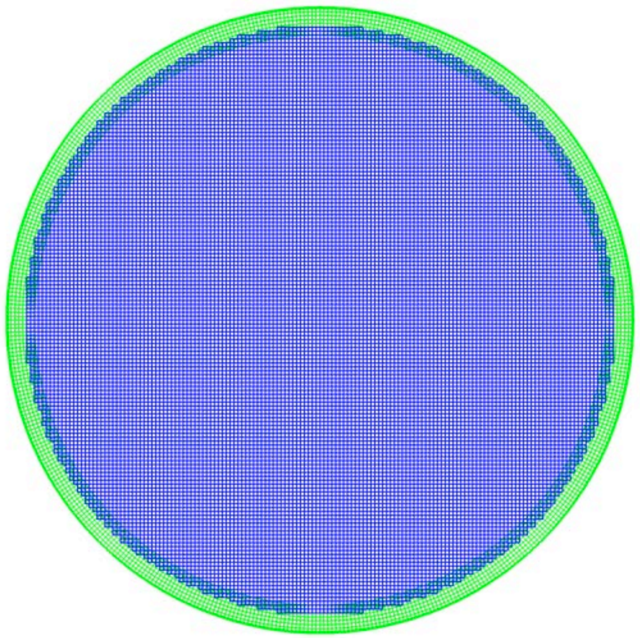

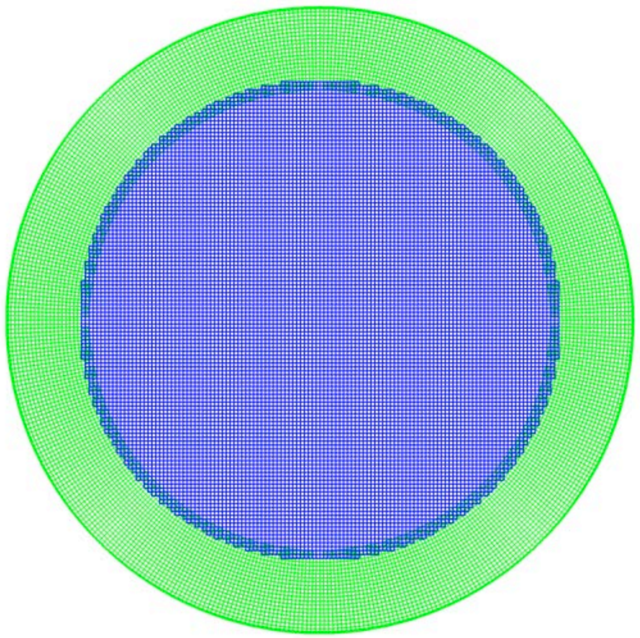

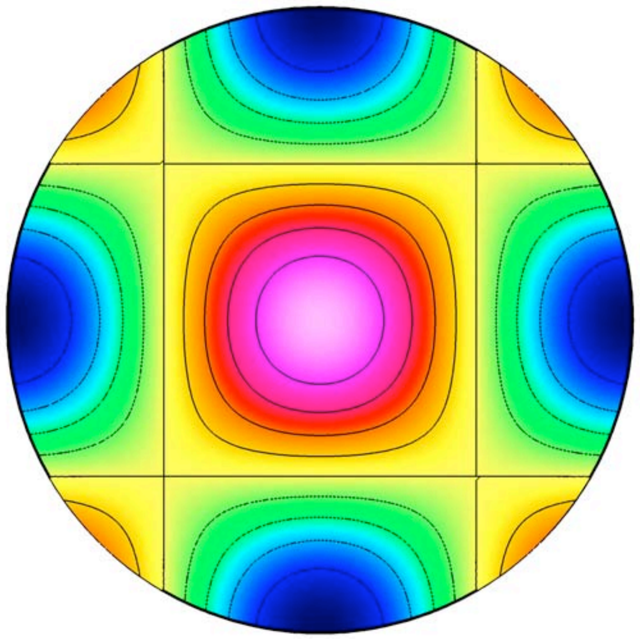

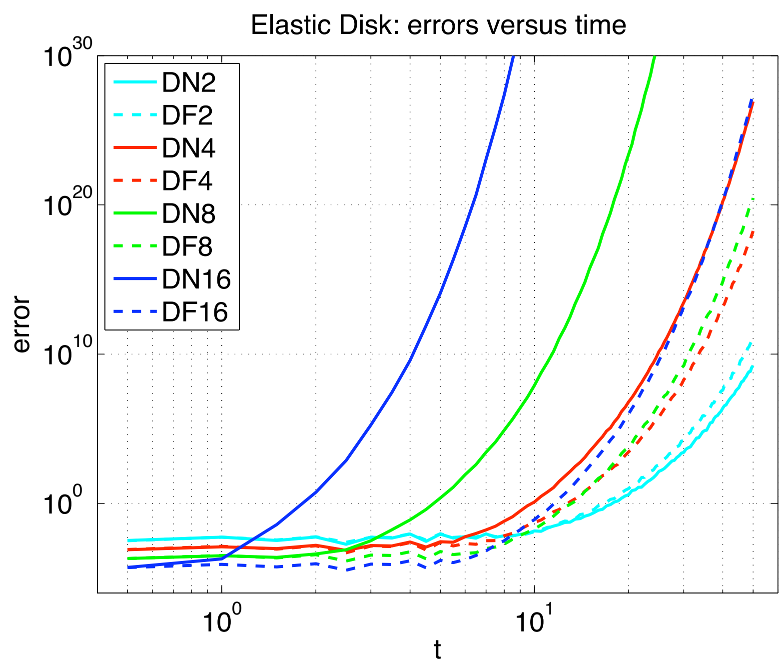

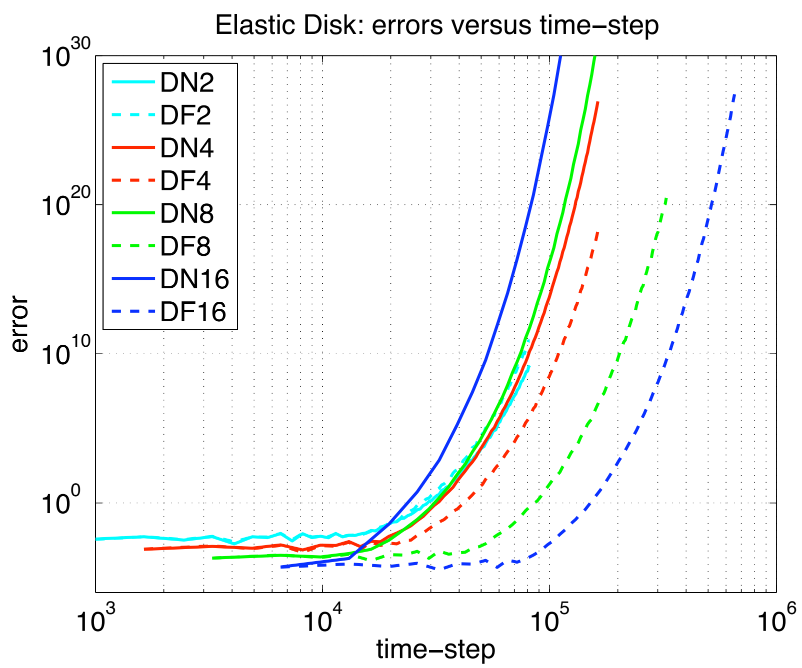

SOS scheme without dissipation

Experiments Concerning Stability

- Consider a planar disk discretized on an overlapping grid (both fixed, and narrow)
- Use method of analytic solutions to generate an exact solution

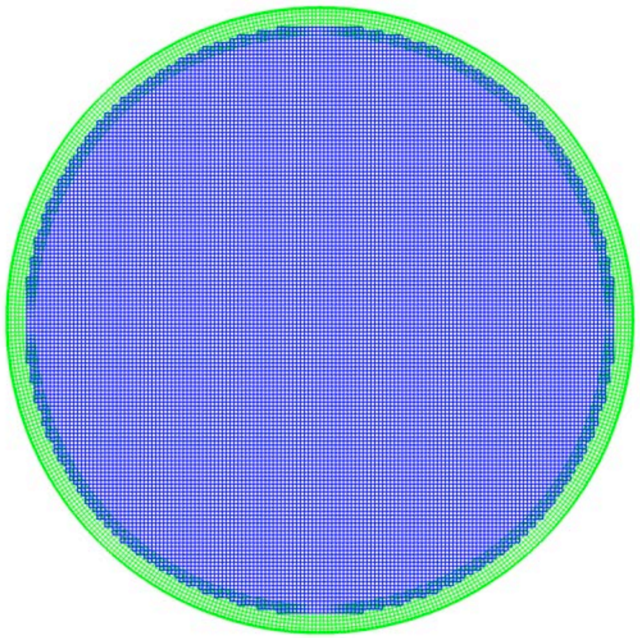

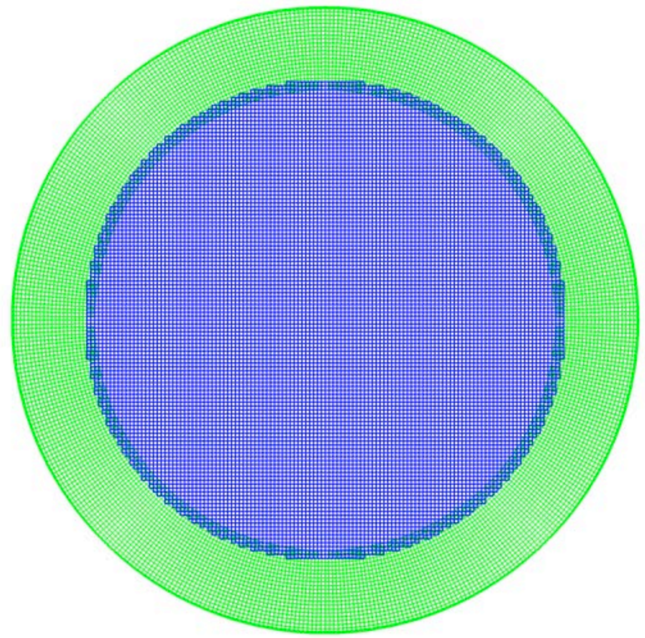

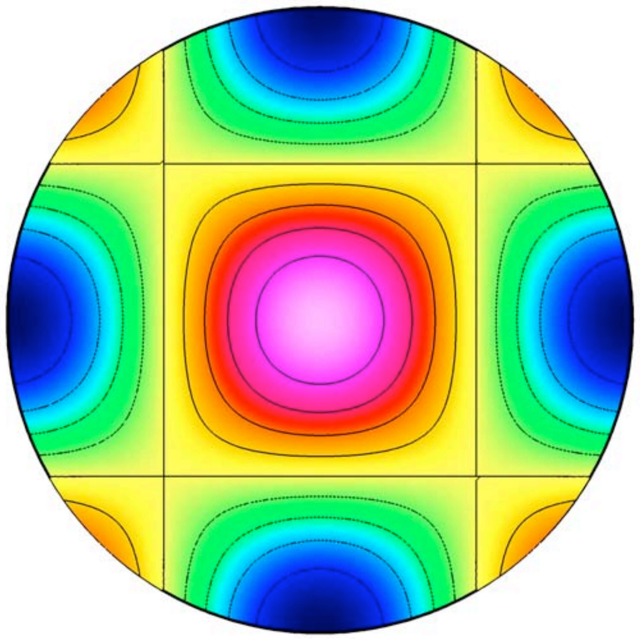

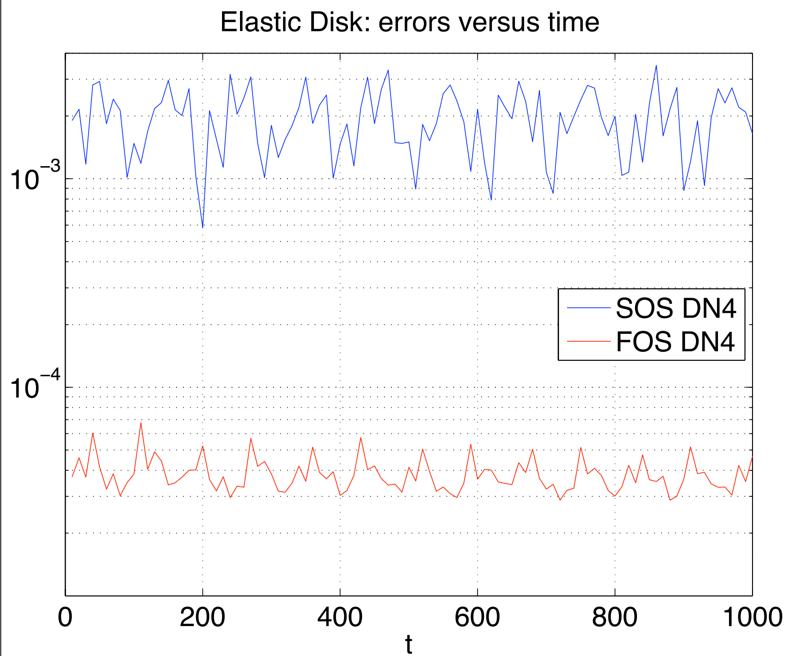

		SOS		FOS					
Grid $\mathcal{G}_{Dn}^{(j)}$	h_j	$e_u^{(j)}$	r	$e_u^{(j)}$	r	$e_v^{(j)}$	r	$e_\sigma^{(j)}$	r
$\mathcal{G}_{Dn}^{(2)}$	$1/20$	5.4×10^{-3}		4.6×10^{-4}		3.1×10^{-3}		3.8×10^{-3}	
$\mathcal{G}_{Dn}^{(4)}$	$1/40$	1.2×10^{-3}	4.4	1.1×10^{-4}	4.3	7.0×10^{-4}	4.5	9.1×10^{-4}	4.2
$\mathcal{G}_{Dn}^{(8)}$	$1/80$	3.1×10^{-4}	3.9	2.9×10^{-5}	3.7	1.7×10^{-4}	4.0	2.3×10^{-4}	3.9
$\mathcal{G}_{Dn}^{(16)}$	$1/160$	7.8×10^{-5}	4.0	7.6×10^{-6}	3.8	4.3×10^{-5}	4.0	5.8×10^{-5}	4.0
rate		2.03		1.97		2.05		2.00	

Vibrations of an Elastic Sphere

- One classic test problem of eigenmode vibrations of a sphere (Lamb 1882, Love 1944)
- Spheroidal vibrations are one such solution (of the *second class*)
- The exact solution for displacements is found as

$$u_j^{(2)} = A_2 \cos(\omega_2 t)\hat{u}_j^{(2)}, \qquad j = 1, 2, 3,$$

$$\hat{u}_1^{(2)} = x_1 \left\{ \frac{1}{\alpha_2^2}\psi_2({}_2) - \frac{1}{2}\left(2x_3^2 - r^2\right)\psi_3({}_2) - C_2\left[\frac{1}{\kappa_2^2}\psi_1(\kappa_2) + \frac{1}{3}\left(8x_3^2 - 7r^2\right)\psi_3(\kappa_2)\right]\right\},$$

$$\hat{u}_2^{(2)} = x_2 \left\{ \frac{1}{\alpha_2^2}\psi_2({}_2) - \frac{1}{2}\left(2x_3^2 - r^2\right)\psi_3({}_2) - C_2\left[\frac{1}{\kappa_2^2}\psi_1(\kappa_2) + \frac{1}{3}\left(8x_3^2 - 7r^2\right)\psi_3(\kappa_2)\right]\right\},$$

$$\hat{u}_3^{(2)} = -x_3 \left\{ \frac{2}{\alpha_2^2}\psi_2({}_2) + \frac{1}{2}\left(2x_3^2 - r^2\right)\psi_3({}_2) - C_2\left[\frac{2}{\kappa_2^2}\psi_1(\kappa_2) + \frac{1}{3}\left(6x_3^2 - 7r^2\right)\psi_3(\kappa_2)\right]\right\},$$

Vibrations of an Elastic Sphere

- One classic test problem of eigenmode vibrations of a sphere (Lamb 1882, Love 1944)
- Spheroidal vibrations are one such solution (of the *second class*)

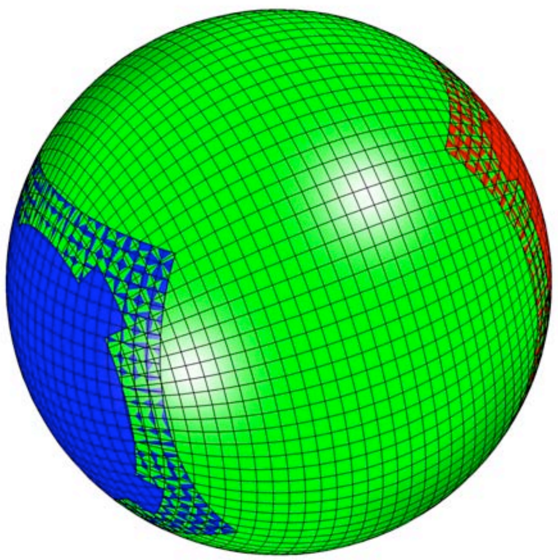

surface grid

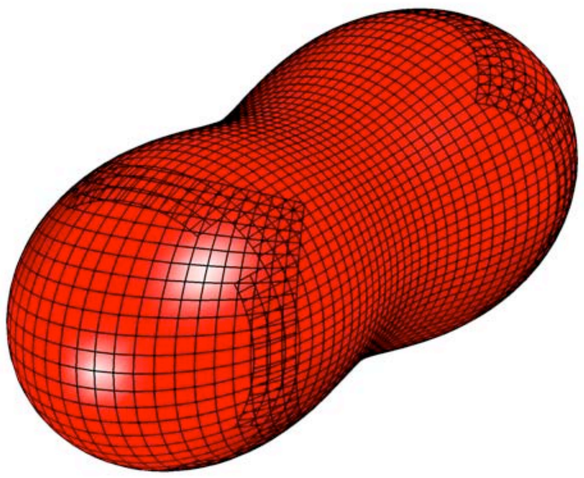

t=0.0

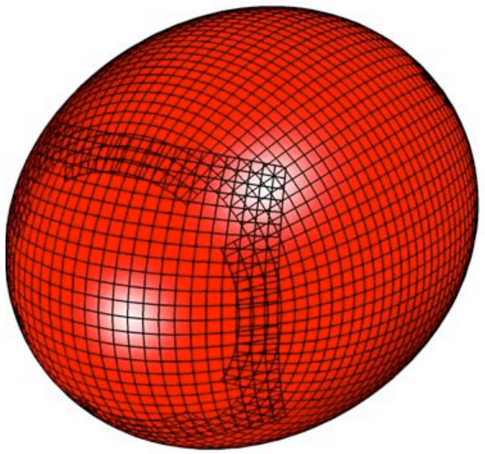

t=0.8

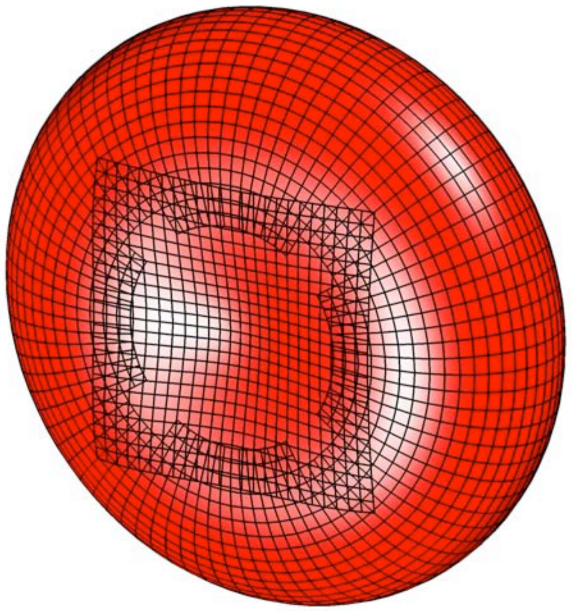

t=1.2

		SOS		FOS					
Grid $\mathcal{G}^{(j)}$	h_j	$e_u^{(j)}$	r	$e_u^{(j)}$	r	$e_v^{(j)}$	r	$e_\sigma^{(j)}$	r
$\mathcal{G}_{ss}^{(1)}$	1/10	1.3×10^{-1}		5.1×10^{-2}		1.2×10^{-1}		2.6×10^{-1}	
$\mathcal{G}_{ss}^{(2)}$	1/20	4.0×10^{-2}	3.2	1.2×10^{-2}	4.2	3.0×10^{-2}	4.0	5.1×10^{-2}	5.1
$\mathcal{G}_{ss}^{(4)}$	1/40	10.0×10^{-3}	4.0	2.4×10^{-3}	5.1	7.1×10^{-3}	4.2	8.6×10^{-3}	6.0
$\mathcal{G}_{ss}^{(8)}$	1/80	2.4×10^{-3}	4.1	5.2×10^{-4}	4.6	1.7×10^{-3}	4.1	2.0×10^{-3}	4.3
rate		1.93		2.22		2.03		2.37	

Adaptive Mesh Refinement

- AMR is a useful addition for many applications
  - In particular fluid structure interaction with shocks
- AMR follows naturally within our overlapping grid framework
- Consider the diffraction of a p-wave "shock" by a cylinder

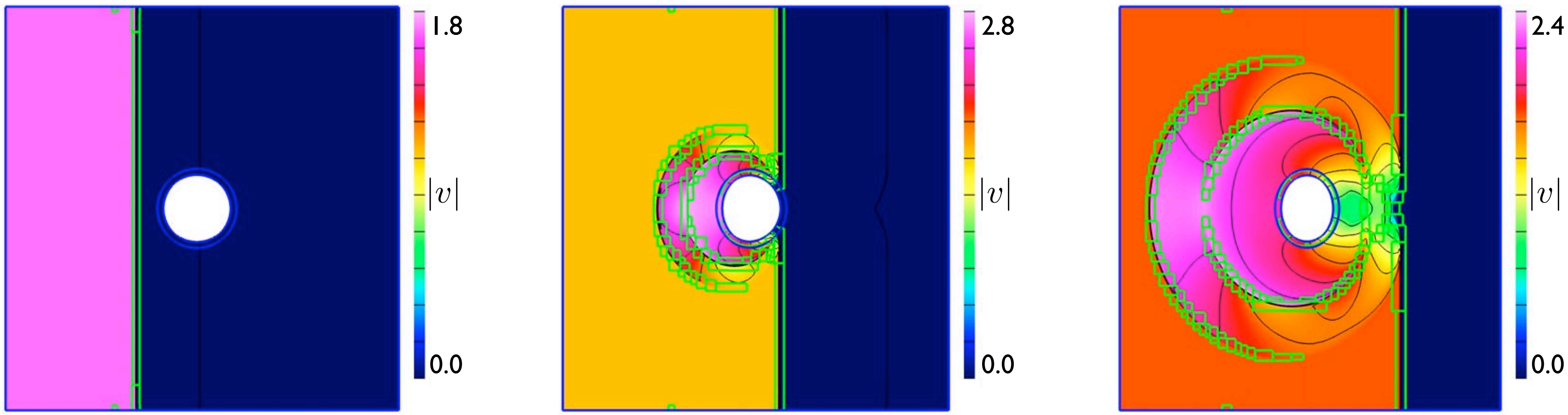

t=0.0 t=1.0 t=1.6

- A posteriori estimates of the error are computed using a series of three computations

				SOS		FOS					
Grid	levels	n_r	h_j	$e_u^{(j)}$	r	$e_u^{(j)}$	r	$e_v^{(j)}$	r	$e_\sigma^{(j)}$	r
$\mathcal{G}_{CS}^{(8)}$	2	2	$1/80$	1.6×10^{-3}		1.6×10^{-3}		5.0×10^{-3}		5.7×10^{-3}	
$\mathcal{G}_{CS}^{(8)}$	2	4	$1/160$	7.3×10^{-4}	2.3	9.0×10^{-4}	1.7	2.3×10^{-3}	2.2	2.6×10^{-3}	2.2
$\mathcal{G}_{CS}^{(64)}$	–	–	$1/320$	3.3×10^{-4}	2.3	5.2×10^{-4}	1.7	1.0×10^{-3}	2.2	1.2×10^{-3}	2.2
rate				1.17		0.79		1.13		1.11	

Circular Plate

- An example of a somewhat more complex situation

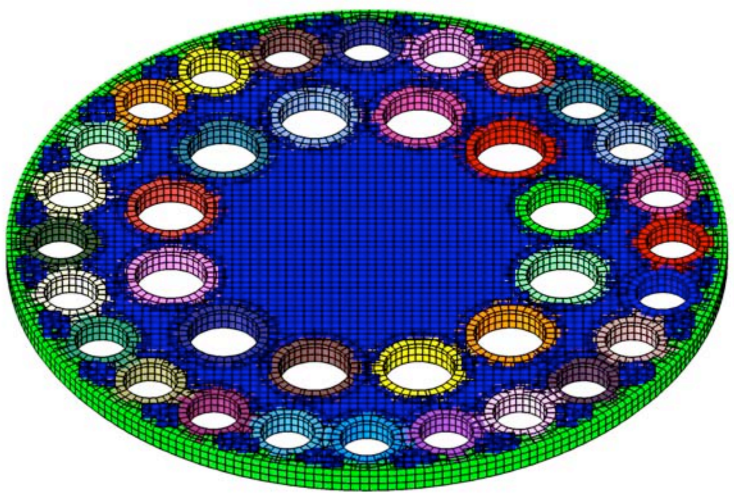

grid

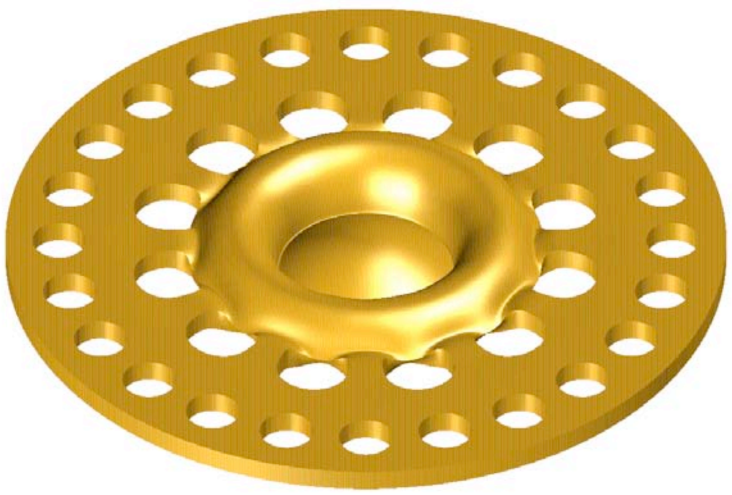

t=2.0

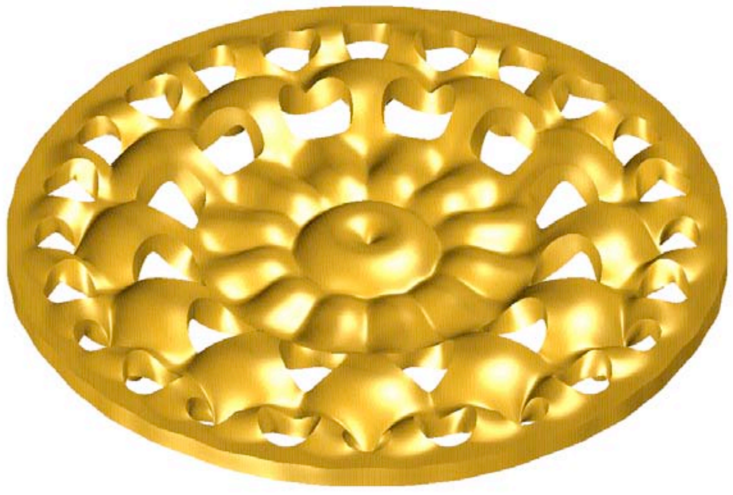

t=4.0

- Again, a posteriori error estimates can be computed from a series of successive grids

		SOS		FOS					
Grid $\mathcal{G}^{(j)}$	h_j	$e_u^{(j)}$	r	$e_u^{(j)}$	r	$e_v^{(j)}$	r	$e_\sigma^{(j)}$	r
$\mathcal{G}_P^{(4)}$	$1/40$	1.8×10^{-2}		9.5×10^{-3}		1.0×10^{-1}		1.3×10^{-1}	
$\mathcal{G}_P^{(8)}$	$1/80$	4.5×10^{-3}	3.9	2.2×10^{-3}	4.2	2.8×10^{-2}	3.6	3.2×10^{-2}	3.9
$\mathcal{G}_P^{(16)}$	$1/160$	1.2×10^{-3}	3.9	5.3×10^{-4}	4.2	7.7×10^{-3}	3.6	8.2×10^{-3}	3.9
rate		2.0		2.1		1.9		2.0	

A Discussion About Relative Performance

- As an example, consider the problem of spheroidal vibrations
- approximately 34 million grid points
- approximately 1.1 million interpolation points
- 16 processors

	Vibration of a Sphere (3D)					
	SOS			FOS		
	total (s)	s/step	%	total (s)	s/step	%
advance	90	1.3	45	2005	16.9	67.
boundary conditions	15	.22	7	51	.42	1.7
interpolation	41	.60	20	876	7.4	29.
filter	40	.58	20	—	—	—
other	5	.10	8	30	.18	2.3
total	190	2.8	100	2962	24.9	100

Performance (cont'd)

	Vibration of a Sphere (3D)					
	SOS			FOS		
	total (s)	s/step	%	total (s)	s/step	%
advance	90	1.3	45	2005	16.9	67.
boundary conditions	15	.22	7	51	.42	1.7
interpolation	41	.60	20	876	7.4	29.
filter	40	.58	20	—	—	—
other	5	.10	8	30	.18	2.3
total	190	2.8	100	2962	24.9	100

- FOS maintains 15 components (could reduce to 12), SOS maintains 3
- FOS is ~12 times more expensive per time step advance
- The FOS time step is smaller by a factor of $\sqrt{3}$
- All told, the FOS scheme is ~16 times slower for a given grid
- However, one grid doubling increases cost by ~16 but decreases error by ~4
- Typical results indicate FOS can be 5-10 times more accurate for a given resolution

Conclusions

- We have developed solid mechanics solvers for overlapping grids
- Solvers based on the both the first and second order systems are investigated
- New stability results for the second order system with overlap
- The performance of the two solvers is compared via a suite of tests

Current and Future Work

- Couple solid mechanics solvers to fluid solvers (in progress)
- Move to nonlinear elasticity as necessary
- Investigate “upwind” solvers for the second order system (in progress)
- Investigate stress relaxation techniques for the first order system (in progress)

Selected References

D. Appelo, J. W. Banks, W. D. Henshaw and D. W. Schwendeman, *Numerical Methods for Solid Mechanics on Overlapping Grids: Linear Elasticity*, SIAM J. Sci. Comput. (submitted)

J. W. Banks and B. Sjogreen, *A Normal Mode Stability Analysis of Numerical Interface Conditions for Fluid/Structure Interaction*, Commun. Comput. Phys. (accepted)

D. W. Henshaw, J. W. Banks and D. W. Schwendeman, *Fluid/Structure Interaction on Overlapping Grids* (in preparation)